ELSEVIER

Polymer 42 (2001) 4885–4892

polymer

www.elsevier.nl/locate/polymer

Effect of molecular structure on dynamic mechanical properties of polyethylene obtained with nickel–diimine catalysts

L.C. Simon[a], R.F. de Souza[a], J.B.P. Soares[b], R.S. Mauler[a,*]

[a]*Instituto de Química, Universidade Federal do Rio Grande do Sul, Av. Bento Gonçalves 9500, Porto Alegre 91501-970, Brazil*
[b]*Department of Chemical Engineering, Institute for Polymer Research, University of Waterloo, Waterloo, Canada N2L 3G1*

Received 3 April 2000; received in revised form 31 July 2000; accepted 5 December 2000

Abstract

Polyethylene made with a nickel–diimine catalyst was studied in order to understand the relationship between molecular structure and dynamic mechanical properties. Different branch lengths, from methyl to longer, and their contents in these ethylene homopolymers, dramatically affects the crystallinity of these polyethylene samples, as shown by differential scanning calorimetry (DSC) and crystallization analysis fractionation (CRYSTAF). T_m and CRYSTAF profiles are related not only to the branch content but also to the distribution on the chain. The dynamic mechanical thermal analysis showed three different groups of materials, where the stiffness varies according to the short-chain branching (SCB) content. Polyethylenes with high SCB showed a strong β-transition (tan $\delta > 1$) despite the lack of any detectable crystallinity. © 2001 Elsevier Science Ltd. All rights reserved.

Keywords: Crystallinity; Polyethylene; Nickel–diimine catalyst

1. Introduction

One of the main advances in the polyolefin technology in the last decade was the use of single-site metallocene catalysts to produce a new variety of ethylene and α-olefinic copolymers [1]. It enables polyolefinic materials to strengthen their presence in the fields of elastomer and plastomer. This is the case of materials such as Engage or Afinity produced by Insite Dow technology [2]. These catalysts permit to improve control of molecular weight (MW), molecular weight distribution (MWD) and short-chain branching (SCB), which can be used to enhance the performance of the final product.

Recently, Du Pont developed the Versipol process, where olefins are polymerized with nickel–diimine complexes as catalyst precursors [3]. These catalysts can make branched ethylene homopolymers in the absence of any α-olefin as comonomer [4,5]. Short-chain branches are produced through the chain walking mechanism, with no comonomer addition, and the degree of branching can be controlled by reaction parameters such as polymerization temperature, ethylene pressure and type of catalyst precursor and co-catalyst [6–8]. ^{13}C NMR studies showed that methyl to hexyl branches, or longer, were produced [9,10], although methyl branches were predominant. A detailed Monte Carlo model has been recently proposed to simulate polymerization and short-chain branch formation with these catalysts [11].

The effect of branching in polyethylene has been studied in detail and it is of crucial importance in understanding and predicting polyolefin properties [12]. The presence of chain branches decreases the size of the linear, crystallizable, sequences in the backbone, i.e. the size of the lamella thickness [13] thus modifying the morphology and the degree of crystallinity [14]. The size of $-CH_2-$ sequences with minimum length to crystallize at a given temperature determines if the lamellar structure is feasible or not. The fringed micelle structure is formed when the methylene sequences are not long enough to form the lamellar structure. Polyolefins containing a very high number of branches are predominantly amorphous although bundled-like crystals might be present [15,16]. It has been also shown that some types of short branches, specially methyl or ethyl, could lead to interstitial lattice imperfection [17–19]. The amorphous phase is also affected by chain branches. Polyethylenes containing branches of at least two carbons had increased concentration of tie-molecules [20], which can be beneficial to properties such as environmental stress crack resistance [21,22].

The dynamic mechanical properties of polyolefins are related to the branch distribution because of its dependence on crystallinity and phase distribution. Below the melting

* Corresponding author. Tel./fax: +55-51-31-66-296.
E-mail address: mauler@if.ufrgs.br (R.S. Mauler).

PII: S0032-3861(00)00917-4

temperature, the polyethylene shows three transitions, or relaxations, designated as α, β and γ, that can be detected by dynamic mechanical thermal analysis (DMTA) [23]. The α-relaxation temperature is associated to modifications in crystalline domains previous to melting and it depends mainly on the crystallite thickness and on the method of crystallization and recrystallization [24]. The interfacial contents, representing a transition layer between the crystalline core and the amorphous domains, are identified by the β-transition [25,26]. This transition is attributed to motions that occur within the interfacial region associated with lamellar crystallites. The γ-relaxation depends mainly on the amorphous content [27], more specifically to the so-called crankshaft mechanism, the relaxation of the hindered rotation of four methylene groups.

Many efforts have been made to correlate molecular structure to mechanical properties in ethylene copolymers [28–30] and in blends of polyolefins [31–33]. In this work, we investigate how the molecular structure of polyethylene made with nickel–diimine catalyst affects its morphology and dynamic mechanical properties.

2. Experimental

2.1. Polymerization

The polyethylene samples were synthesized using a nickel–diimine catalyst precursor, with triisobutylaluminum or trimethylaluminum as cocatalyst, in homogeneous polymerization reactor using chlorobenzene as solvent. Polymerization conditions were: ethylene pressure of 1.08 atm, temperature of −20, 0 or 30°C, 80 ml of chlorobenzene, 10 μmol of nickel complex, 1,4-bis(2,6-diisopropyphenyl)-acenaphthenediimine-dichloro-nickel(II), and aluminum to nickel molar ratio of 200. More detailed information was published elsewhere [8].

2.2. ^{13}C NMR

The polymer microstructure was qualitatively and quantitatively analyzed by ^{13}C nuclear magnetic resonance (NMR) spectroscopy. The branches were classified as methyl, ethyl, propyl, butyl, pentyl and hexyl + (hexyl and longer) according to previous work [9]. The spectra was obtained with a Varian Inova 300 spectrometer operating at 75 MHz, at 80 or 120°C, with a 71.7° flip angle, acquisition time of 1.5 s and delay of 4.0 s. Sample solutions of the polymer were prepared in *o*-dichlorobenzene and benzene-d_6 (30% w/v) in a 5-mm tube.

2.3. Gel permeation chromatography

The molecular weight (MW) was evaluated by gel permeation chromatography (GPC) with the Waters 150CV system equipped with three columns Styragel HT3, HT4 and HT6 (10^3, 10^4 and 10^6 Å, respectively) and a refractive index detector. Analyses were undertaken using 1,2,4-trichlorobenzene as solvent (with 0.5 g/l of Irganox 10/10 as antioxidant) at 140°C and the MWs were calculated using a universal calibration curve built with polyethylene, polypropylene and polystyrene standards (American Polymer Standard Corporation).

2.4. Crystallization analysis fractionation

Crystallization analysis fractionation (CRYSTAF) was performed using the Polymer ChAR CRYSTAF 200 equipment. Approximately 5 mg of sample was dissolved in 30 ml of 1,2,4-trichlorobenzene used as solvent (with 0.5 g/l of Irganox 10/10 as antioxidant). Sample dissolution was done at 160°C for 30 min followed by 60 min of equilibrium period at 95°C. The crystallization rate was 0.1°C/min from 95 to 10°C. The CRYSTAF 200 equipment was cooled below room temperature with liquid nitrogen.

2.5. Film preparation

Differential scanning calorimetry (DSC) and dynamic mechanical thermal analysis (DMTA) data were evaluated from films. Polyethylene films were prepared in a Carver press Monarch series, model 3710 ASTM. The polymers were pre-heated for 2 min at 160°C between the press plates without pressure and then pressed by 2 min at 3 kgf/cm^2 at the same temperature. After this time, the pressure was released and the films were controlled cooled down to room temperature at the cooling rate of 10 or 1°C/min, or quenched in water-ice bath or liquid nitrogen. The film thickness was 0.15 mm ± 0.02.

2.6. Differential scanning calorimetry

A Thermal Analyses DSC 2010 calorimeter was used to determine melting temperatures. Discs cut out from films were heated in closed pans from room temperature to 160°C, held at this temperature for 4 min, cooled down to −150°C, and then heated again to 160°C. The heating and cooling rates were 10°C/min. The analyses were performed under nitrogen flux. Melting point temperatures and degree of crystallinity were determined in the second scan. Degree of crystallinity (λ_c), was calculated from the DSC traces using the enthalpies of fusion of the perfectly crystalline polyethylene (293 J/g [34]).

2.7. Dynamic mechanical thermal analysis

The dynamic mechanical tests were done using the MK II DMTA Polymer Laboratories instrument operating in the tensile mode. The sample dimensions were $0.15 \times 7.0 \times 12$ mm^3. Measurements were taken at 1 Hz. The temperature was raised from −150 to 150°C at a scanning rate of 2°C/min.

Table 1
Properties of polyethylenes made with nickel–diimine catalyst. (T_m, melting temperature in DSC; λ_c, degree of crystallinity evaluated by DSC; T_γ, γ relaxation peak at DMTA; T_β, β relaxation peak at DMTA, $T_{\alpha'}$,$_\alpha$: α relaxation peak at DMTA; T_C, CRYSTAF distribution peak)

Sample	$M_w \times 10^{-3}$ (g/mol)	M_w/M_n	Cooling rate (°C)	T_m (°C)	λ_c	T_γ (°C)	T_β (°C)	$T_{\alpha'}$ (°C)	T_α (°C)	T_C (°C)
A	329	1.5	−10	124	0.54	−107	−6	–	99	80.8
Ai			Ice[a]	124	0.49	− 109	–	–	74	–
B	184	2.1	−10	118	0.41	−107	−16	–	86	74.5
C	142	1.5	−10	120	0.52	−107	–	–	90	75.7
D	470	2.1	−10	84	0.27	−113	−17	–	–	42.1
E	354	2.1	−10	75	0.44	−120	−30	–	–	32.7
F	619	2.3	−10	86	0.50	−110	−15	12	–	45.8
Fa			−1	88	0.42	−116	−22	32	–	–
Fi			Ice[a]	83	0.25	−115	−20	67	–	–
Fn			$N_{2(L)}$[b]	89	0.38	−115	−21	–	–	–
G	161	2.2	−10	–	0	−116	−58	–	–	–
H	137	2.2	−10	–	0	−113	−60	–	–	–

[a] Sample quenched in ice-water bath.
[b] Sample quenched in liquid nitrogen.

3. Results and discussion

3.1. Chain microstructure

The polyethylene samples studied herein had different SCB distribution, which led to distinct thermal and dynamic mechanical properties. Table 1 shows some properties for these polyethylenes and Table 2 presents a more detailed microstructure characterization by ^{13}C NMR.

Sample B contained only methyl branches, while others samples had methyl and longer branches. However, the following pattern of distribution was found: 1,4-separated methyl, 1,5-separated methyl, 1,6-separated methyl and 1,4-separated long branches. The 1,4-separated methyl nomenclature, for example, indicates the relative position of the next neighbors to the branch in the backbone, in this case a methyl branch separated from other branches by two $-CH_2-$ units [9]. The other branch types (methyl, ethyl, propyl, and so on) were assumed to be randomly distributed along the backbone [11]. The backbone of samples with low methyl branch content was similar to that of ethylene–propylene random copolymers. The backbone of the high-branched samples, H or G, had a singular structure, which would be similar to that of copolymers of ethylene and mixtures of α-olefins.

3.2. Crystallinity

The difference in SCB produced materials with distinct thermal responses and morphology. Some samples had a well-defined melting peak while others had a broad melting transition. The highly branched samples did not have a melting transition. The melting temperatures (T_m), crystalline contents (λ_c) and melting ranges observed with DSC for the several polyethylene samples are shown in Table 1. Fig. 1 shows selected DSC traces. The experimental uncertainty in measuring the transition temperature during DSC was smaller than 0.2°C while crystalline contents reported here have uncertainty of ±6%.

As the SCB increases, the linear sequences get shorter and cause the polymer to crystallize at lower temperatures and in smaller, less perfect structures, affecting the morphology [35]. The broad melting ranges presented in samples D and E can be attributed to a broad distribution of lamella thickness.

In crystallization analysis fractionation (CRYSTAF), the polymer chains crystallize from dilute solution. Cocrystallization effects and chain entanglement, commonly present in DSC, do not affect CRYSTAF analyses to a significant extent. Fig. 2 shows CRYSTAF curves from selected samples. The crystallization peak temperature (T_C) observed with CRYSTAF is also shown in Table 1.

Samples A, B and C had higher T_Cs, indicating a low SCB. This was in agreement with SCB content obtained by ^{13}C NMR, as indicated in Table 2. Sample A had the crystallization peak temperature at 80.8°C, which was close to the temperature of linear polyethylene ($T_C = 85$°C) [36].

Table 2
Short chain branch distribution in polyethylene made with nickel–diimine catalyst analyzed by ^{13}C NMR (branches per 1000 C in the backbone)

Branch	Sample						
	B	C	D	E	F	G	H
Methyl (total)	12.9	13.3	30.7	33.3	34.4	55.4	66.6
Methyl-1,4	1.0	0.4	4.0	2.3	8.5	18.4	25.3
Methyl-1,5	0	0	0	0	0	6.9	8.8
Methyl-1,6	0	0.2	14.5	6.0	14.5	12.8	16.6
Ethyl	0	0.4	4.5	4.9	5.4	10.1	13.8
Propyl	0	1.3	1.3	6.9	5.4	10.6	3.7
Butyl	0	0.2	2.8	2.8	3.0	11.1	11.1
Pentyl	0	0	0	0	0	3.5	3.5
Hexyl and longer (Bn)	0	0	1.7	0	0	16.8	16.8
1,4-Bn	0	0	2.3	0	0	3.2	7.0
Total branched carbons	12.9	15.2	42.6	48.0	48.1	107.5	121.5

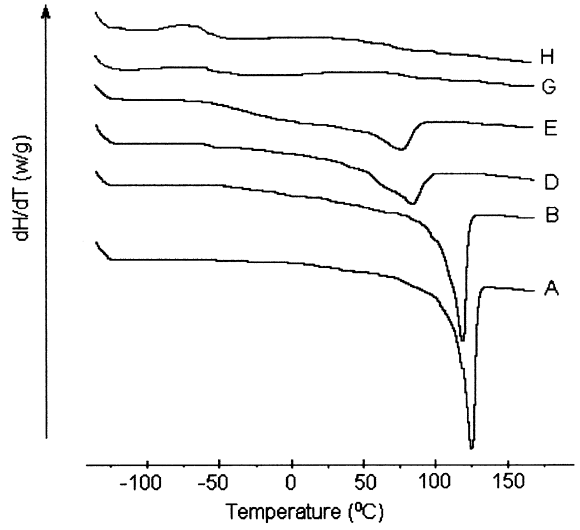

Fig. 1. Melting traces runs of nickel–diimine catalyzed polyethylenes.

Although the branch content of sample A was not measured by ^{13}C NMR, its higher T_C (in CRYSTAF) and higher T_m (in DSC) than sample B suggest that sample A has fewer branches than sample B. Samples B and C had a narrow distribution of SCB distribution with T_cs centered at 74.5 and 75.7°C, respectively. Although both samples B and C had a similar SCB distribution, they did not have the same CRYSTAF profiles. The CRYSTAF curve of sample C was narrower than that of sample B and the peak is located at a higher temperature. However, the differences of molecular weight and polydispersity between samples B and C (Table 1) are small and such effect is believed to be minimal in CRYSTAF because crystallization occurs from diluted solution [37]. The difference in CRYSTAF profiles of samples B and C is attributed to different SCB distribution in these polyethylene samples.

The broad CRYSTAF traces of samples F and D and the tails indicate that these samples had a less uniform interchain SCB distribution. Sample E had a narrower distribution than F, but the total number of branched carbons was the same. Probably, the differences observed in the CRYSTAF profiles among samples D, E and F are related to the methyl branch distribution (Table 2). Sample E had methyl branches distributed more separately than the other two samples D and F because the number methyl-1,4 and methyl-1,6 branches were considerably smaller in sample E (17%) than in samples D (43%) and F (48%) affording longer methylenic segments and, consequently, higher T_C.

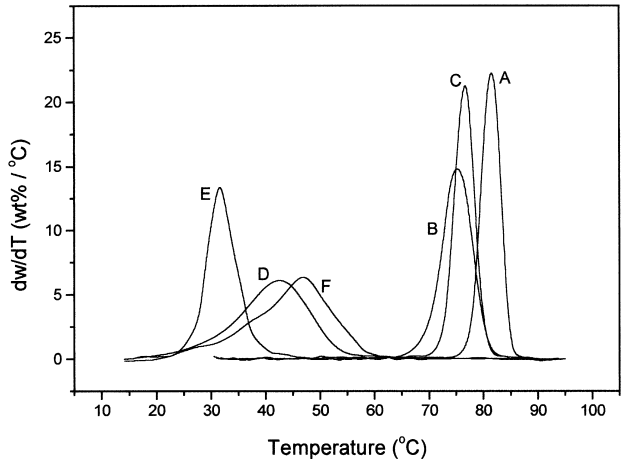

Fig. 2. Crystallization analysis fractionation profiles of nickel–diimine catalyzed polyethylenes.

CRYSTAF gives information about the composition heterogeneity because its profiles are related to the distribution of crystal thickness [38,39]. Polymer chains precipitate from solution at a given temperature as a function of the length of their longest methylene sequence. The understanding of the interchain compositional heterogeneity has been shown to be of extreme importance to explain the mechanical behavior, like fracture toughness of linear low-density polyethylene [40].

DSC and CRYSTAF for the samples with high SCB (G and H) failed to give useful information about SCB distribution. DSC traces showed a transition in the range of −60 to 10°C approximately. Some authors have identified such transition as being the second glass transition temperature in ethylene copolymers [41]. In these polyethylenes, the length of crystallizable methylene sequences were not uniform due to the diversity of chain branches and their distribution. It produced a very broad distribution of crystal thickness that caused a broadening of the melting peak and, in more limited cases, the formation of an extremely large or even not detectable melting peak. No CRYSTAF peak could be seen because the samples did not crystallize within the experimental temperature range used for crystallization.

3.3. Dynamic mechanical properties

The storage moduli measured with DMTA are shown in Fig. 3. Below −50°C, all samples had nearly the same stiffness, with storage modulus varying from 10^9 to 10^{10} Pa. Above −50°C, the real part of the modulus could be separated, according to stiffness, in three different groups.

The moduli of the samples with low SCB content (A and B) decreased from −50 to 130°C and the values were in the range of linear polyethylene, i.e. around 10^8 Pa. For the samples D and E, the storage modulus decreased from 10^9 Pa, at −50°C, to less than 10^7 Pa at about 100°C. These values covered the range from linear low-density polyethylenes to very low-density polyethylenes made with Ziegler–Natta or metallocene catalysts [42,43]. One can see, from the above comparison, that an increment of SCB content had the effect of an efficient plasticizer [44]. Samples G and H, with highest SCB, showed a deep change in the storage modulus, from 10^9 Pa at −50°C to 10^6 Pa, around 50°C, far below of values commonly seen for very low-density polyethylenes.

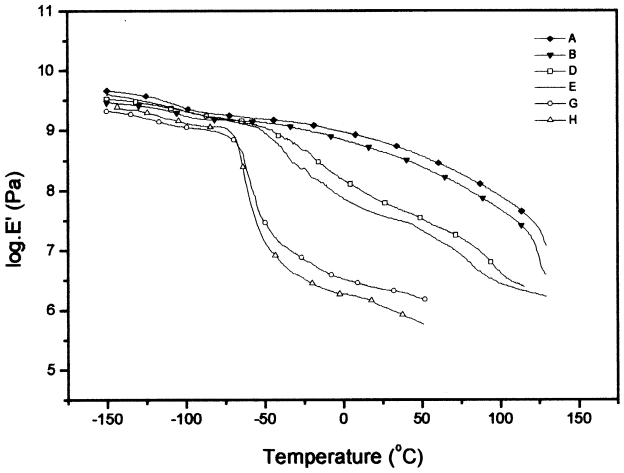

Fig. 3. Storage moduli (E') of nickel–diimine catalyzed polyethylenes.

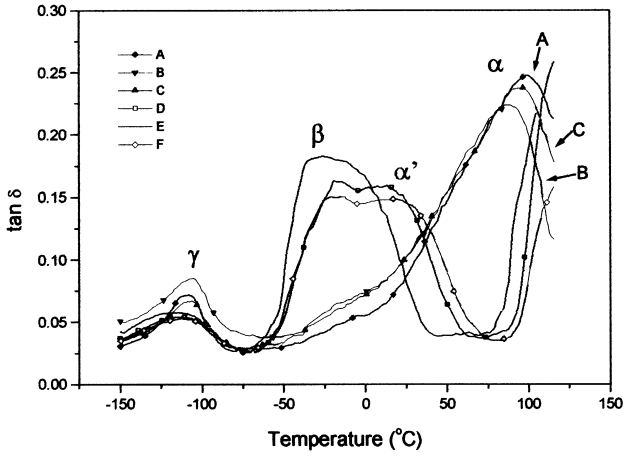

Fig. 4. Mechanical damping (tan δ) of nickel–diimine catalyzed polyethylenes. The α, β and γ-transitions.

The α-, β- and γ-transitions [45] can be seen when the mechanical damping (tan δ) is plotted against temperature. The peak temperatures, T_α, T_β and T_γ corresponding to each transition, respectively, are shown in Table 1.

The γ-transition is mainly an amorphous-phase relaxation process [27]. At the molecular level, it is attributed to the relaxation of hindered rotation of $-CH_2-$ groups in the amorphous phase [46]. The tan δ traces (Fig. 4) showed that the γ-transition temperature (T_γ) was nearly the same for all samples. It had the onset at −120°C and finished at −106°C. Samples with smaller SCB content (A, B and C) had a more intense γ-transition. An increment in the SCB content decreased the linear $-CH_2-$ segments available to take part in the rotation process [47]. In Fig. 5, the tan δ traces of samples with high SCB, G and H, are compared to the sample D. One can see that the γ-transition did not decrease in intensity with increasing SCB content. Indeed, samples G and H had branches with up to six carbons or more, which could contribute to the intensity of γ-relaxation. A Monte Carlo simulation of the SCB distribution predicted that branches longer than six carbons must be present in these samples altogether [11]. This may suggest that in these high-branched samples (G and H), the carbon atoms from branches with more than six carbon atoms would be contributing to increase the γ-transition intensity.

The β-transition has been related to diffusional motion of amorphous chain segments containing branch points and that the branch points cooperate with main and side chain groups on that motion [50]. More recently, the β-transition has been attributed to segmental motions occurring within the crystal–amorphous interfacial regions [26]. It is also known that an increment in the number of side chain branches increases the β-transition intensity [44]. In samples with low number of SCB (A–C), the β-transition appeared with low intensity and as a weak shoulder in the α-transition peak (see Fig. 4).

The α-transition was related to segmental motion within crystals prior to melting [23,24]. It was also reported for low-density polyethylene having branches longer than hexyl [48]. Samples A–C, with low SCB, showed a marked α-transition. The differences observed between the α-transition on samples A–C may be attributed to differences in MW and methyl branch distribution.

Sample E, with 48 branches per 1000 carbons (48 branches/1000 C), showed a marked β-transition. The tan δ curves of sample D and F showed similar behaviors between −75 and 75°C (Fig. 4), with a β-transition (left peak) superimposed onto another transition (right peak). The second peak observed might be due to α'-transition. The presence of two α-relaxations is attributed to motions within crystallites of different lengths from those giving rise to the α-transition [26,28,44]. Samples E and F had approximately the same number of branches according to ^{13}C NMR data (Table 2). The difference observed in the β-transition might be attributed to the difference in branching distribution for these samples (see CRYSTAF curve in Fig. 2).

The β-transition of samples G and H appeared as an intense and sharp peak at −58 and −60°C, respectively. This is observed by comparing the tan δ traces of samples G and H to the trace of sample D in Fig. 5. These T_β were shifted to lower temperatures than the T_β of other samples and their intensity decreased with the increment of SCB content. Samples H and G had the highest SCB content among the samples studied here, with 121.5 and 107.5 branches/1000 C, respectively. Popli showed that the intensity of the β-transition is substantially increased by raising the interfacial content [24]. DSC and CRYSTAF failed to detect the T_m and T_C, respectively, in samples G and H.

Copolymers of ethylene and α-olefins synthesized using metallocene catalytic systems, which produce an uniform branch distribution, have shown similar behavior in terms of α-, β-, and γ-transition [49]. Sample A had the T_α and the intensity of α-transition similar to that of ethylene homopolymer made with metallocene catalyst. The β-transition of samples E and F (ca 50 branches/1000 C) were less intense than the β-transition showed by ethylene/1-octene

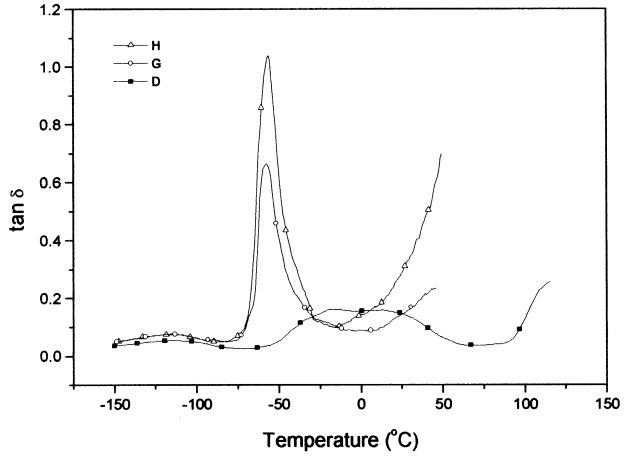

Fig. 5. Mechanical damping (tan δ) of nickel–diimine catalyzed polyethylenes.

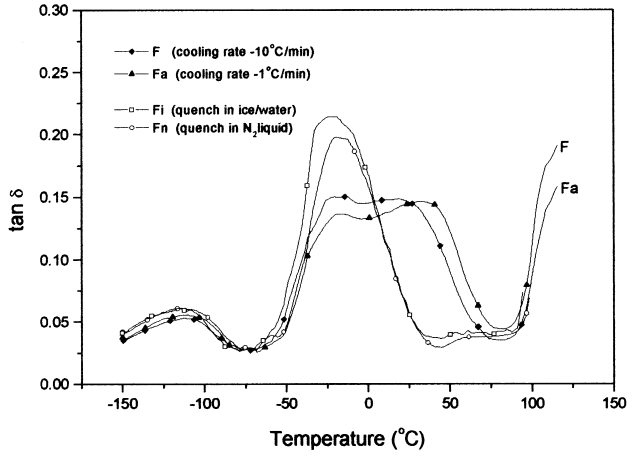

Fig. 6. Mechanical damping (tan δ) of nickel–diimine catalyzed polyethylenes. The effect of thermal treatment in films over β and α'-transition.

or 1-decene (10% mol or ca 50 branches/1000 C) and T_β of samples E and F were higher than for the ethylene copolymers, since close branches make the $-CH_2-$ longer and consequently leading to a higher T_C.

Boyer has interpreted the β-transition as the upper glass transition, $T_g(U)$, occurring in amorphous debris arising from imperfect chain folding action. This transition was displaced to lower temperatures when the crystallinity was decreased and appeared at −78°C for the total amorphous polyethylene [50]. The β-transition reported in this work followed the same trend. However, the materials without crystallinity (G and H) had the β-transition peak at −60°C (Table 1).

The above discussion concludes that understanding the nature of β-relaxation is a fundamental point to correlate structure–property, but the true mechanism remains unclear. The β-transition seems to be related to branched-point relaxations indeed, either if they are related to an interfacial phase or to a low-oriented phase.

3.4. Thermal treatment

Polymer response to thermal treatment is important to determine the properties and to find both the conditions to process the material and the appropriate final use. The importance of temperature-cooling rate over polymer morphology is well known [51]. The effect of thermal treatment was studied with samples A and F using films prepared in different cooling rates or quenching. The new samples Fa, Fi and Fn were prepared from polymer F and the sample Ai was prepared from polymer A. For samples Ai and Fi, the melted films were quenched on a ice-water bath. In the sample Fn, the melted film was quenched in liquid nitrogen. For sample Fa, the melted film was cooled down to room temperature (30°C) at the rate of −1°C/min. These different thermal treatments were compared to the one done for the others samples (including samples A and F) where these films were cooled down to room temperature at the rate of −10°C/min. The cooling rates and DMTA results are shown in Table 1.

Fig. 6 shows the tan δ traces of sample F submitted to different thermal treatments. The thermal treatment did not affect the onset of α-transition for samples F and Fa, which were controlled cooled down from the melt. However, samples F and Fa had the α-transition with higher intensity than samples Fi and Fn (quenched samples), probably because the slow cooling allowed crystals to grow. The γ-transition appeared to be more intense in both quenched samples indicating the presence of more amorphous phase.

The intensity of β-transition on samples of family F was notably affected by thermal treatment although the onset of β-transition had not been affected. Between −75 and 80°C, the tan δ of sample Fa had the same two peaks present in sample F, the β-transition (left peak) and the α'-transition (right peak). Furthermore, the temperature of α'-transition was higher and such transition was more intense in samples Fa than in sample F. The quenched samples Fi and Fn had a lack of α'-transition but a more intense β-transition peak. It

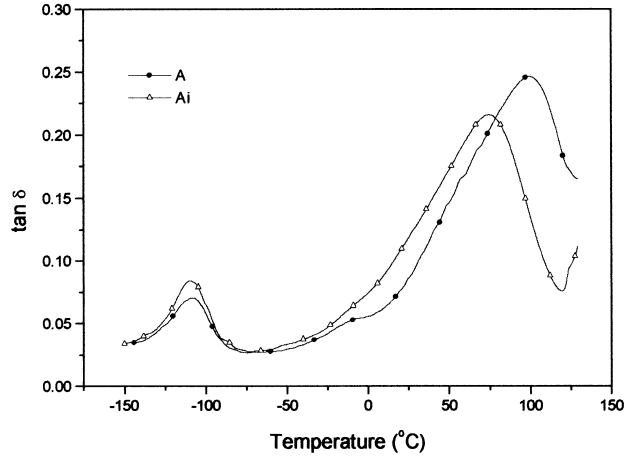

Fig. 7. Mechanical damping (tan δ) of nickel–diimine catalyzed polyethylenes. The effect of thermal treatment in films over α-transition.

is clear that the dynamic mechanical properties were strongly affected by the thermal treatment and likely the interfacial phase present in sample F.

Other authors reported that measurements of mechanical properties on polyethylene with less than 21 SCB per 1000 carbons submitted to thermal treatment (slow cooled or quench) did not change enough the crystallinity to affect the transitions in the mechanical properties [29].

In samples with low SCB content (A–Ai), the thermal treatment changed both the peak position and the intensity of α-transition. Sample A had the peak at 99°C while sample Ai (quenched in ice-water bath) had the peak at 74°C. The β-transition, in samples of family A, appeared as a small shoulder in the α-transition peak, see Fig. 7. The γ-transition appeared to be more intense in the quenched polyethylene indicating that more chains were trapped in amorphous regions during the rapid process of freezing.

4. Conclusions

The polyethylenes obtained with nickel–diimine catalyst can cover a broad range of properties, varying among plastics, plastomers and elastomers. The main reason for different properties is the differences in microstructure due to short chain branching (SCB) content.

The values of storage modulus (E') ranged from values of linear polyethylene to below the values of very low-density polyethylene.

The tan δ traces of samples with low methyl branch content (<20 branches/1000 C) showed the β-transition as a small shoulder in the α-transition. In samples with medium SCB content (ca 50 branches/1000 C), two superimposed transitions could be seen between −75 and 75°C attributed to the β-transition and the α'-transition. Thermal treatment of these samples may affect the distribution of material among amorphous, interfacial and crystalline domains.

The high-branched polyethylene (>100 branches/1000 C) did not develop detectable crystallinity. They showed a strong and sharp transition in the temperature range of β-transition, exhibiting rubbery character.

Acknowledgements

We thank FAPERGS, CAPES and CNPq for financial support.

References

[1] Montagna AA, Burkhart RM, Dekmezian AH. Chemtech 1997;December:26.
[2] Batistini A. Macromol Symp 1995;100:137.
[3] Johnson LK, Killian CM, Brookhart M. US Patent 96/23010, 1996.
[4] Johnson LK, Killian CM, Brookhart M. J Am Chem Soc 1995;117:6414.
[5] Brookhart M, Johnson LK, Killian CM, Mecking S, Tempel DJ. Polym Prepr 1996;37(2):254.
[6] de Souza RF, Mauler RS, Simon LC, Nunes FF, Vescia DVS, Cavagnolli A. Macromol Rapid Commun 1997;18:795.
[7] Schleis T, Spaniol TP, Okuda J, Heinemann J, Mülhaupt R. J Organometal Chem 1998;569:159.
[8] Simon LC, de Souza RF, Mauler RS. J Polym Sci Part A Polym Chem 1999;37:4656.
[9] Galland GB, de Souza RF, Mauler RS, Nunes FF. Macromolecules 1999;32:1620.
[10] Jurkiewicz AA, Eilerts NW, Hsieh ET. Macromolecules 1999;32:5471.
[11] Simon LC, Soares JBP, de Souza RF. AIChE J 2000;46:1234.
[12] Mandelkern L. J Phys Chem 1971;75:3909.
[13] Flory PJ. J Am Chem Soc 1962;84:2857.
[14] Glotin M, Mandelkern L. Macromolecules 1981;14:1394.
[15] Minick J, Moet A, Hiltner A, Baer E, Chum SP. J Appl Polym Sci 1995;58:1371.
[16] Bensason S, Minick J, Moet A, Chum S, Hiltner A, Baer E. J Appl Polym Sci 1996;34:1301.
[17] Swan PR. J Polym Sci 1962;56:409.
[18] Vonk CG, Pijepers AP. J Polym Sci Polym Phys Ed 1985;23:2517.
[19] McFaddin DC, Russell KE, Kelusky EC. Polym Commun 1986;27:204.
[20] Mathur SC, Mattice W. Macromolecules 1988;21:1354.
[21] Lustiger A, Markham RL. Polymer 1983;24:1647.
[22] Huang Y-L, Brown N. J Polym Sci Part B Polym Phys 1991;29:129.
[23] Boyd RH. Polymer 1985;26:1123.
[24] Rault J. J Macromol Sci Rev Macromol Chem Phys C 1997;37(2):335.
[25] Popli R, Mandelkern L. Polym Bull 1983;9:260.
[26] Popli R, Glotin M, Mandelkern L. J Polym Sci Part B Polym Phys 1984;22:407.
[27] Gray RW, McCrum NG. Polym Sci A2 1969;7:1329.
[28] Simanke AG, Galland GB, Freitas L, da Jornada JAH, Quijada R, Mauler RS. Polymer 1999;40:5489.
[29] Brooks NWJ, Duckett RA, Ward IM. Polymer 1999;40:7367.
[30] Simanke AG, Galland GB, Baumhardt Neto R, Quijada R, Mauler RS. J Appl Polym Sci 1999;74:1194.
[31] Loss J, Bonnet M, Petermann J. Polymer 2000;41:351.
[32] Mader D, Thomann Y, Suhm J, Mulhaupt R. J Appl Polym Sci 1999;74:838.
[33] Rana D, Cho K, Woo T, Lee BH, Choe S. J Appl Polym Sci 1999;74:1169.
[34] Runt JP. Crystallinity determination. In: Mark HF, Bikales NM, Overberger CG, Menges G, Kroschwitz J, editors. Encyclopedia of polymer science and engineering, vol. 4. New York: Wiley-Interscience, 1986. p. 487.
[35] Mathot VBF, Scherrenberg RL, Pijpers TFJ. Polymer 1998;39:4541.
[36] Silva Filho AA, Soares JBP, Galland GB. Macromol Chem Phys 2000;201:1226.
[37] Defoor F, Groeninckx, Schouterden P, Van der Heijden B. Polymer 1992;33:5186.
[38] Monrabal B. J Appl Polym Sci 1994;52:491.
[39] Monrabal B. Macromol Symp 1996;110:81.
[40] Mirabella Jr FM, Westphal SP, Fernando PL, Ford EA, Williams JG. J Polym Sci Part B Polym Phys 1988;26:1995.
[41] Reding FP, Faucher JA, Whitman RD. J Polym Sci 1962;57:483.
[42] Khanna YP, Yuri EA, Taylor TJ, Vickroy V, Abbott R. Macromolecules 1985;18:1302.
[43] Starck P. Eur Polym J 1997;33(3):339.
[44] Clas S-D, McFaddin DC, Russell KE. J Polym Sci Part B Polym Phys 1987;25:1057.
[45] Oakes WG, Robinson DW. J Polym Sci 1954;14:505.

[46] Schatzki TF. J Polym Sci 1962;57:494.
[47] Kline DE, Sauer JA, Woodward AE. J Polym Sci 1956;22:455.
[48] Orozco JAG, Rego JM, Katime I. J Appl Polym Sci 1990;40:2219.
[49] Simanke AG, Galland GB, Freitas LL, da Jornada JAH, Quijada R, Mauler RS. Macromol Chem Phys 2001 (in press).
[50] Boyer RF. J Macromol Sci Phys B 1973;8:503.
[51] Androcsh R, Wunderlich B. Macromolecules 1999;32:7238.